COMPENSATION FOR TIME-DEPENDENT STAR TRACKER THERMAL DEFORMATION ON THE AQUA SPACECRAFT

Joseph A. Hashmall[1,2], Gregory Natanson[1], Jonathan Glickman[1], and Joseph Sedlak[1]

[1] a.i. solutions,Inc.,10001 Derekwood Lane, Lanham MD 20706, USA
[2] E-mail: hashmall@ai-solutions.com

ABSTRACT

Analysis of attitude sensor data from the Aqua mission showed small but systematic differences between batch least-squares and extended Kalman filter attitudes. These differences were also found to be correlated with star tracker residuals, gyro bias estimates, and star tracker baseplate temperatures. This paper describes the analysis that shows that these correlations are all consistent with a single cause: time-dependent thermal deformation of star tracker alignments.

These varying alignments can be separated into relative and common components. The relative misalignments can be determined and compensated for. The common misalignments can only be determined in special cases.

1. INTRODUCTION

The Aqua spacecraft was launched on May 4, 2002 into a nearly circular, sun-synchronous, polar orbit. Primary attitude sensors consisted of two Charge-Coupled Device (CCD) Star Trackers (ST). These sensors, together with an inertial reference unit (IRU)—also referred to as gyros, are designed to maintain the spacecraft at an Earth-pointing attitude with an attitude knowledge requirement of 25 arcsec (3σ) on all axes.

The National Aeronautics and Space Administration (NASA) Goddard Space Flight Center (GSFC) Aura flight dynamics attitude team had the responsibility of verifying that the onboard attitude system was achieving the required accuracy. For Aura the attitude validation using a ground batch least-squares (BLS) algorithm showed significant attitude differences (on the order of ±15 arcsec). This paper discusses identification of the source of these differences.

Section 2 describes the observations that led to the ultimate conclusion that the attitude differences were due to a thermally-induced variation in the star tracker alignments. Section 3 presents analysis that isolates the time-dependent misalignments into relative and common components. This section shows how the relative misalignments may be compensated, what the effects of this compensation are, and why compensation for the common misalignments is more difficult. Section 4 summarizes the results and presents conclusions that will affect subsequent similar missions (for example Aura).

2. OBSERVATIONS

Attitude validation is normally accomplished by comparing ground BLS with onboard extended Kalman filter (EKF) attitude solutions. The ground solutions are considered more accurate because:

- a larger star catalog is used
- more complete star identification algorithms are available
- star position corrections (such as for velocity aberration and precession) can be used
- a more accurate, post-facto definitive ephemeris is used.

For Aqua, differences between onboard and ground attitude solutions varied in a range of about ±15 arcsec [1-4]. These differences appeared to repeat with a period similar to the orbital period (about 6000 seconds). Fig. 1 compares the EKF and BLS attitudes over a period of three orbits.

All plots of EKF data in this paper were computed using a ground EKF. The cited references show that the results of the ground EKF are almost identical to those of the onboard EKF. The data used were from a three day period (19-21, June 2003).

Initial analysis attempted to determine if the observed attitude differences were caused by a change in gyro bias. The gyro bias variation was presumed to be thermally induced. Variations in gyro bias would appear as differences between EKF and BLS solutions because the BLS algorithm assumes a constant gyro bias over the batch, whereas the EKF estimates time-varying biases.

The gyro biases were found to vary regularly with a period of several orbits. In initial studies, the repeat

period was 4-orbits but with later data it reduced to 3-orbits!

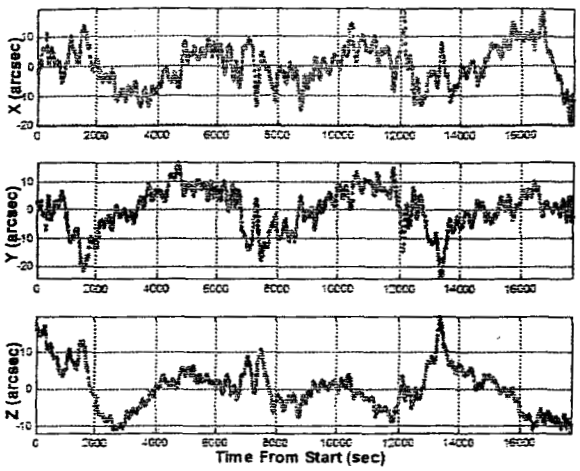

Fig. 1. Attitude Differences Between EKF and BLS Aqua Attitudes Over a Three Orbit Period

To model these periodic variations in Aqua measurements, a parameter referred to as "3-orbit phase" was developed. The 3-orbit phase is identical to orbit phase but continues to increase for three satellite revolutions (from 0 to 1080 degrees (deg)). Fig. 2 shows the computed X-, Y-, and Z-gyro biases plotted against 3-orbit phase.

The data used in this analysis were taken from a 3-day continuous span of Aqua observations. This span covers 44 full orbits and represents almost 15 separate cycles of 3-orbit phase. The data (in this case gyro bias) were grouped in bins within a range of 3-orbit phases. The range was generally 1 deg. For each bin, the corresponding value is calculated as the mean of all samples within the bin, and the uncertainties as the standard deviations over the samples within the same bin.

Thus, each point in Fig. 2 represents the mean of all computed gyro biases at the corresponding 3-orbit phase in bins of 1 deg. Superimposed on these values are error bars representing their standard deviations. The repeatability of the biases is striking.

Fig. 3 shows the corresponding residuals from star tracker 1. The residuals are defined as the vector difference between the body frame star tracker measurements and the star tracker reference vectors, converted into the body frame using the current attitude estimate. The star trackers have a square, 8-deg. field-of-view (FOV) and are situated with their boresight unit vectors approximately [0.67 0.66 -0.34] and [-0.67 0.66 -0.34] in the body frame.

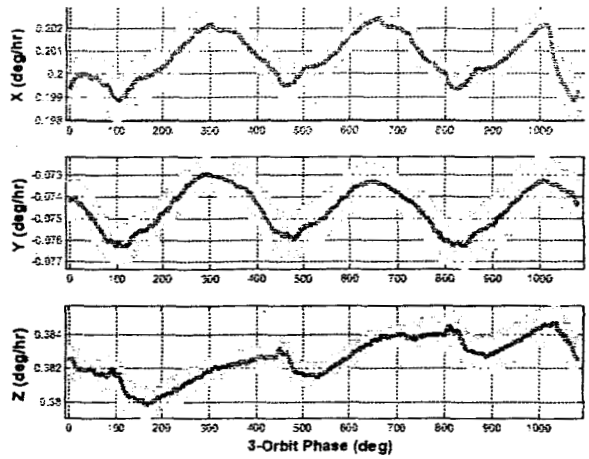

Fig. 2. Mean and Uncertainty of EKF Gyro Biases as Functions of 3-Orbit Phase

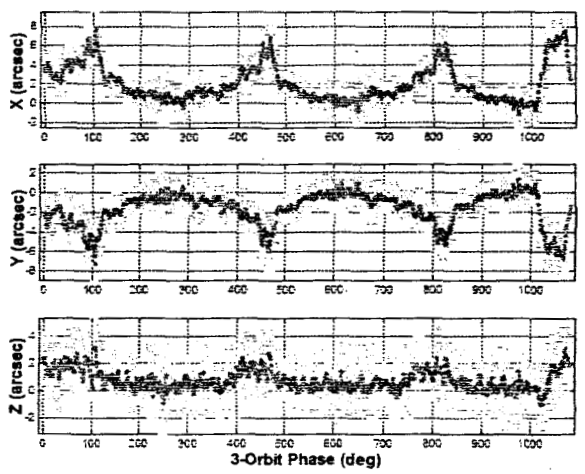

Fig. 3. Mean and Uncertainties of Star Tracker 1 Residuals Biases as Functions of 3-Orbit Phase

The systematic patterns in biases, residuals, and attitude differences, were not due to variation of the gyro temperatures. A temperature sensor at the IRU showed no significant temperature variations. In contrast, a temperature sensor at the star tracker baseplate showed exactly the pattern of variation shown by the gyro biases. Fig. 4 shows these temperatures plotted against orbit phase, in the upper portion, and against 3-orbit phase, in the lower portion. All observed temperatures at 8 second intervals are included in this figure as dots (•). The width of the "lines" is indicative of the variability of temperatures that occur at the same 3-orbit phase.

The 3-orbit repeat time of the pattern arises from activation of a heater. In each orbit the star tracker baseplate temperature increases during the sunlit portion of the orbit and decreases in darkness. Superimposed on this periodic variation is a constant decrease in temperature. When the temperature falls below a threshold (at orbit phase of about 300 deg in the third orbit) a heater is activated, raising the

temperature to the starting point of the cycle. Early in the mission, the secular cooling trend was slower and the heater activated only every 4 orbits. This explains the change from a 4-orbit cycle to a 3-orbit cycle. Because the star trackers are not directly exposed to the Sun, there is a lag time in the heating and cooling.

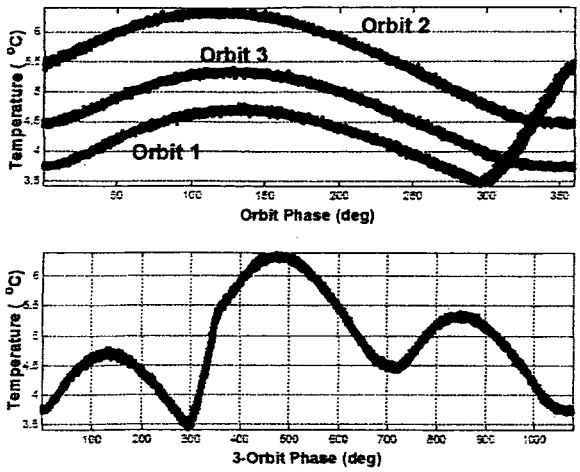

Fig. 4. Star Tracker 1 Baseplate Temperatures (deg C) as Function of Orbit Phase and 3-Orbit Phase

The origin of the 3-orbit phase representation is arbitrary. Here, it is consistently defined so that the orbit in which the heater is activated has 3-orbit phase from 0 to 360 deg.

Similar patterns can be found in examining the star tracker residuals and the differences between EKF and BLS attitudes. The patterns are less apparent because of random variations in the properties compared. Analysis was performed in an attempt to understand the cause of these variations.

The coincidence of the pattern of star tracker baseplate temperature and variations in gyro biases, sensor residuals, and attitude differences must be causal. However, there is no simple correlation between temperature and any of the observed parameters.

The following analysis shows that variation in star tracker alignment explains all of these observations. The alignment variation is expected to be a function of secular and spatial temperature gradients in addition to the temperature.

3. ANALYSIS

Temperature variations can easily cause alignment shifts. If the star tracker alignments change, the residuals (differences between observed and reference star vectors) will not be consistent with gyro measurements. The effect of this inconsistency on the filter is to cause a change in the solution. The change will be distributed between the attitude and the gyro bias depending on how the filter is tuned.

To better understand the details of the effect of sensor misalignment changes on attitude and gyro bias solutions, it is useful to separate misalignments into two types: relative misalignments and common misalignments.

Relative misalignments are misalignments that change the relative position of two sensors but do not change their mean positions. Common misalignments are misalignments that change the positions of two sensors together, so that their relative position remains the same but their mean position changes. Individual changes in alignment of two sensors can always be expressed as changes in relative and common misalignments.

3.1 Relative Misalignments

Relative misalignments can be directly observed and computed using attitude independent algorithms. The 3-day span of Aqua data investigated was divided into periods during which the spacecraft moved 5 deg. of orbit phase (about 82 seconds). During each of these periods, the AliCal [5] algorithm was used to compute the relative misalignment of the two star trackers. The solutions for common 3-orbit phases were averaged and the standard deviations of the samples computed. Fig. 5 shows the resulting mean relative misalignments for tracker 1 and their associated uncertainties.

The misalignments in Fig. 5 are plotted in a mean boresight frame. This frame is defined so that its Z-axis is the mean of the two tracker boresights and its Y-axis the cross product of the two boresights. In this frame, the relative misalignment (which changes the separation of the boresights) is primarily a rotation about the Y-axis. Vectors in the mean-boresight frame are indicated by the subscript "m".

Relative misalignments of two sensors have equal magnitudes and opposite signs in the mean coordinate system so only tracker 1 misalignments are shown. Misalignment components corresponding to rotations around the Y_m-axis result in sensor measurement residuals in the two sensors that are also equal in magnitude and opposite in sign. These residuals influence the attitude determination system in opposite directions and produce no net attitude change and no net EKF bias change.

Misalignment components corresponding to rotations around X_m produce Z_m changes in attitude and EKF biases while misalignments around Z_m produce X_m attitude and EKF bias changes. All components of the relative misalignment reduce sensor residuals.

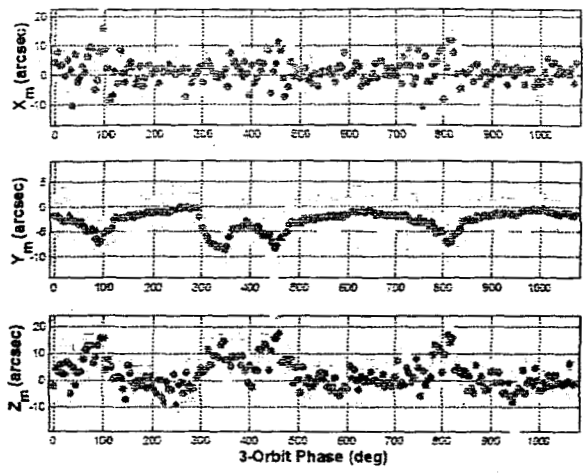

Fig. 5. Mean-Boresight Frame Tracker 1 Misalignments vs. 3-Orbit Phase

The calculated misalignments can be applied in a number of ways. The three most common are to apply half of the relative misalignment to each tracker, keeping the mean unchanged in the body frame. Alternatively, the entire misalignment can be applied to either tracker alone, keeping the unaltered tracker unchanged in the body frame.

Placing equal amounts of misalignment on each tracker compensates for relative misalignment. Placing all of the misalignment on one tracker also compensates for relative misalignment but, in addition, causes a shift of the common misalignment.

Fig. 6 shows the effect of these misalignment compensations on the X-axis gyro bias. The effects on the other gyro biases are similar.

Comparison of the top plot in Fig. 6 (misalignments applied to both trackers) with the top plot in Fig. 2 (X-axis) shows that compensation for relative misalignment does not significantly remove the pattern of gyro biases. In Fig. 6 the gyro bias pattern is more difficult to see because in addition to other sources of noise, the applied misalignments have a sizeable uncertainty.

The change in the pattern of gyro biases seen in the lower 2 plots of Fig. 6 is due to compensation for common misalignment and will be discussed below.

Similar results are obtained for attitude differences as shown in Fig. 7. This figure shows the differences in between attitudes computed with no misalignment compensation, with those compensated in three ways. Application of relative misalignments to both trackers (top plot in Fig. 7) results in only small attitude differences. The Z-axis was chosen for this figure because the pattern of attitude changes (see Fig. 1) is most distinct.

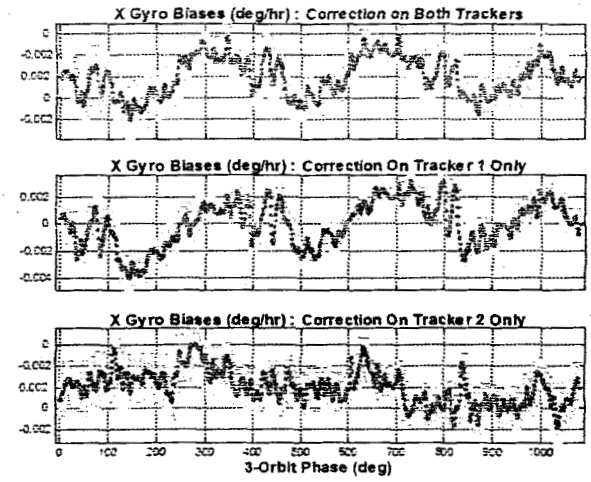

Fig. 6. X-Axis Gyro Biases After Compensation for Relative Misalignment

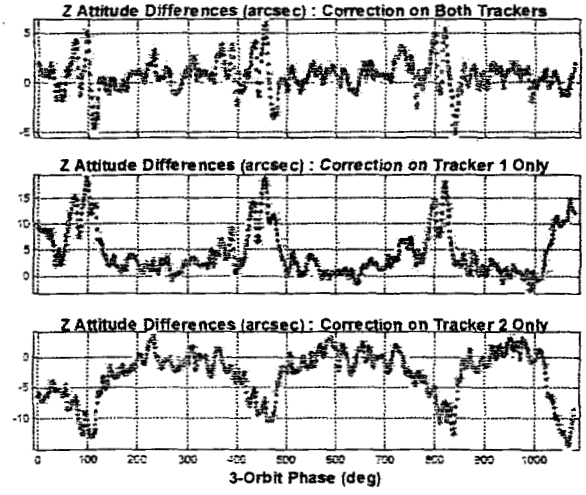

Fig. 7. Z-Axis Differences Between Attitudes Before and After Compensation for Relative Misalignment

In contrast to the lack of changes in attitude and gyro biases, the tracker residuals are changed greatly by removal of the relative misalignment. These changes are illustrated in Fig. 8 for the X-axis residuals in tracker 1. All axes on both trackers show comparable results. The pattern of variation in residuals has almost completely disappeared as compared to that in Fig. 3. This result is produced regardless of how the relative misalignments are applied.

Considering only the case with both trackers compensated for relative misalignment (and therefore with unchanged common misalignment), the results shown in Figs. 6-8 can be easily explained. The EKF responds solely to gyro measurements and sensor error signals (the differences between expected and measured sensor values). When the relative misalignments are compensated to an equal extent on both trackers, the tracker error signals will decrease. This decrease will be about the same size, but

opposite in sign, on the trackers. Thus, the effect of the decreased residuals input to the EKF from one tracker will be nearly exactly compensated by the decreased residuals from the other tracker. The output of the EKF (biases and attitudes) will be almost unchanged.

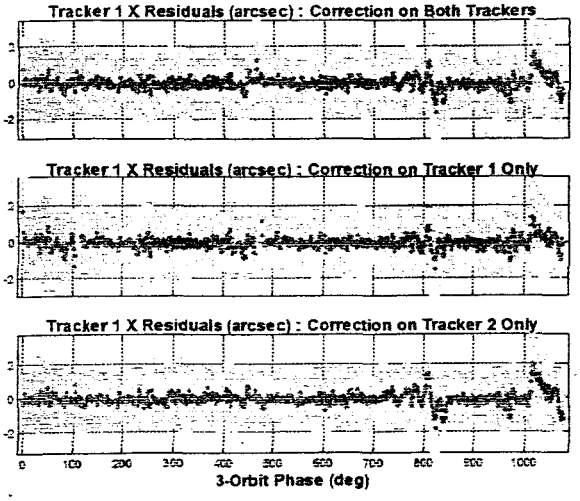

Figure 8. X-axis Star Tracker 1 Residuals After Compensation for Relative Misalignment

3.2 Common Misalignments

When the relative misalignments are compensated, an attempt can be made to evaluate the changes in common misalignments as a function of time. If the common misalignment of the trackers varies, the measured gyro bias and attitude may also vary.

If the biases obtained after compensation for relative misalignment are compared (see Fig. 6), it is found that the bias computed after compensating the two trackers equally is nearly identical to the mean of the biases obtained by compensating each tracker separately. Compensating the two trackers equally does not change the common misalignment. Compensating them separately changes the common misalignment in equal and opposite ways. It is therefore evident that the variation in biases is due to change in common misalignment.

The spacecraft's control system is designed to keep the spacecraft Z-axis pointing towards the Earth. It causes the spacecraft to rotate approximately -0.06 deg/second (ω_s) around the Y-axis. The star trackers provide the only knowledge of the spacecraft attitude, so their common movement changes the axis about which this rotation occurs. The rotation is controlled with respect to a frame based on the star trackers but varies in the body frame because of the time-varying common-misalignment of the trackers.

Assuming the gyro alignment does not change with respect to the body frame, the spacecraft rotation axis will move relative to the gyros. The measured gyro rates will reflect spacecraft rotation about a time-dependent body axis. Neglecting the responsiveness of the onboard attitude determination and control, the attitude will always be controlled to nominal, and the inconsistent measured gyro rates will be compensated for principally by time-varying gyro biases (this compensation will depend on the "tuning" of the EKF).

The transformation from the body frame to the tracker frame can be represented by a time-dependent Euler rotation vector of $[\phi_x, \phi_y, \phi_z]^T$. The transformation from the tracker to the body frame is represented by $[-\phi_x, -\phi_y, -\phi_z]^T$ and the rotation rate in the tracker frame by $[0, \omega_s, 0]^T$. Using e to represent the components of the unit vector from these Euler rotation vectors, and Φ to represent its magnitude, the projection of ω_s on the body axes is given by:

$$\omega_p = \begin{bmatrix} e_x e_y(1-\cos\Phi) - e_z \sin\Phi \\ \cos\Phi + e_y^2(1-\cos\Phi) \\ e_y e_z(1-\cos\Phi) + e_x \sin\Phi \end{bmatrix} \omega_s \qquad (1)$$

For small rotations, an excellent approximation of Eqn. (1) is:

$$\omega_p \cong \begin{bmatrix} -\phi_z \\ 1 \\ \phi_x \end{bmatrix} \omega_s \qquad (2)$$

In addition to detecting the projections of the large rate, ω_s, gyros detect rates due to the movement of the body by the control system in order to keep the time varying star tracker frame pointed nominally. These rates are just the time derivatives of the negative of the common misalignments. The total measured gyro rates, including true biases, b_0, are approximately:

$$\omega_g \cong \begin{bmatrix} -\phi_z \\ 1 \\ \phi_x \end{bmatrix} \omega_s - \begin{bmatrix} \dot{\phi}_x \\ \dot{\phi}_y \\ \dot{\phi}_z \end{bmatrix} + \begin{bmatrix} b_{x0} \\ b_{y0} \\ b_{z0} \end{bmatrix} \qquad (3)$$

The bias computed by the EKF will be the difference between the gyro measured rate and the rate in the tracker frame. These are controlled to be: $[0, \omega_s, 0]^T$.

In the ideal case, EKF biases are approximately:

$$b_x = b_{x0} - \omega_s \phi_z - \dot{\phi}_x \qquad (4)$$

$$b_y = b_{y0} - \dot{\phi}_y \qquad (5)$$

$$b_z = b_{z0} + \omega_s \phi_x - \dot{\phi}_z \qquad (6)$$

If the common misalignments have the same approximate magnitudes as the relative misalignments, they have a range on the order of 10 arcsec. From Fig. 2 it is apparent that misalignments can change over this range in about 1000 seconds. The terms $\dot{\phi}$ and ϕ are therefore similar in magnitude and neither can be ignored.

Even if none of the terms in Eqns. (4-6) are negligible, Eqn. (5) should be relatively simple to solve for ϕ_y if the true bias is known. In this case the y-misalignment at any time, t, is given by:

$$\phi_y(t) = \int_0^t \left(b_y - b_{y0}\right) dt \qquad (7)$$

It is also possible to approximately solve the coupled differential equations (4) and (6). Such a solution requires knowledge of the true biases and the x- and z-misalignment angles at the initial time.

Attempts to solve these equations produced results that were inconsistent with the observations. The solutions for ϕ_y were not periodic, while those for ϕ_x and ϕ_z, although periodic, increased in magnitude with time.

The explanation of this failure arises from any of a number of approximations including that of optimum EKF tuning. Tuning changes how the effect of the tracker residuals is partitioned between attitude and bias changes. For Eqns. (4-6) to be valid, the EKF biases must represent the entire effect of the common misalignment change. This condition implies that the tracker data must be considered extremely reliable.

For Aqua, large vibrations occur due to the operation of the payload instruments. These vibrations produce the equivalent of significant noise on tracker measurements. In turn, this large noise term prevents accurate integration of the equations.

Despite the failure to integrate Eqns. (4-6), some conclusions can be made about the common misalignment. If the entire relative misalignment is applied to tracker 2, the pattern seen in the gyro biases (see Fig. 6) is much less evident than if the misalignments are applied solely to tracker 1. Applying the misalignment to tracker 2 moves the mean of the trackers towards tracker 2. Clearly the common misalignment has a similar effect.

4. CONCLUSIONS

The Aqua spacecraft displayed larger than expected differences between ground and onboard attitude estimates. These differences have a periodic nature and are accompanied by periodic changes in gyro biases and star tracker residuals. They are caused by thermal changes in tracker alignments.

The thermal changes in star tracker alignment resulted in periodic variations in calculated gyro biases, attitude differences, and sensor residuals. The time-varying relative misalignments can be determined and compensated, but computation of the common misalignments is more difficult. Compensation for the relative alignment changes reduces the sensor residuals but has little effect on the attitude or gyro biases.

Although the attitude variations accompanying these alignment shifts are within Aqua specifications, there have been some concerns about the Aura mission (which has a virtually identical platform). The payload instruments on Aura may be more sensitive to attitude deviations than those on Aqua. Several operational possibilities have been discussed for Aura including raising star trackers temperatures and reducing their temperature variation.

5. ACKNOWLEDGEMENTS

The authors acknowledge the support of the National Aeronautics and Space Administration (NASA), Mission Operations and Missions Services (MOMS) Contract NNG04DA01C, Task Order 88, under which this work was performed.

6. REFERENCES

1. J. A. Hashmall and G. Natanson, *Analysis of Aqua Star Tracker Misalignment and Gyro Bias*, CSC, August 2003

2. J. Hashmall, J. Glickman, G. Natanson, and J. Sedlak, *Aqua Onboard Vs. Ground Attitude Discrepancy Analysis*, CSC, May 2003

3. J. Glickman, J. Hashmall, G. Natanson, J. Sedlak, and D. Tracewell, "Earth Observing System-PM1 (EOS-PM1) / Aqua Launch and Early Orbit Attitude Support Experiences", *2003 Flight Mechanics Symposium*, NASA CP-2003-212246, October 2003

4. G. Natanson and J. A. Hashmall, *Effect of Temperature-Dependent Variation of Aqua Star Tracker Relative Misalignments on Attitude Accuracy*, NASA EOS-Attitude Analysis Report-0304-17, CSC, March 2004

5. Hashmall, J.A., and Sedlak, J.E., "New Attitude Sensor Alignment Calibration Algorithms," *53rd International Astronautical Congress*, Houston, TX, IAF, Oct. 2002.